

# Structural assessment of the EU-DEMO water-cooled lead lithium central outboard blanket segment adopting the sub-modelling technique

I. Catanzaro<sup>a,\*</sup>, G. Bongiovì<sup>a</sup>, P.A. Di Maio<sup>a</sup>, P. Arena<sup>b</sup>, G.A. Spagnuolo<sup>c</sup>

<sup>a</sup> Università degli Studi di Palermo, Viale delle Scienze, Edificio 6, 90128 Palermo, Italy

<sup>b</sup> ENEA, Department of Fusion and Nuclear Safety Technology, C.R. Brasimone, 40032 Camugnano (BO), Italy

<sup>c</sup> EUROfusion Consortium, Programme Management Unit, Garching, Germany

## ARTICLE INFO

### Keywords:

WCLL  
Breeding blanket  
Sub-modelling  
Thermomechanics  
FEM analysis

## ABSTRACT

The development of a sound conceptual design of the Water-Cooled Lead Lithium Breeding Blanket (WCLL BB) is pivotal to make a breakthrough towards the selection of the driver blanket concept for the EU-DEMO. To achieve this goal, an intense research campaign has been performed at the University of Palermo, in cooperation with ENEA Brasimone, under the umbrella of EUROfusion. In this paper, structural analyses of different poloidal regions of the WCLL BB Central Outboard Blanket (COB) segment are reported. In particular, starting from the results of the thermo-mechanical analysis of the whole WCLL BB COB segment, the sub-modelling technique has been applied to the most significant poloidal regions, located at the top, middle and bottom of the segment. The aim is to focus on the stress field locally arising under purposely selected steady-state nominal and accidental loading scenarios. The nominal BB operating conditions, as well as steady-state scenarios derived from both the in-box LOCA and Vertical Plasma Disruption accidents have been considered. Thanks to the sub-modelling approach, the deformative action of the entire segment can be imposed at the boundaries of each local model to realistically assess its structural performances. Moreover, each local model reproduces structural details not included in the global one, such as the Segment Box (SB) cooling channels. Then, the structural behaviour of the selected regions has been assessed in compliance with the RCC-MRx code. The obtained results highlighted that the structural behaviour predicted by the whole segment analysis is similar to that predicted by sub-modelling calculations within the Stiffening Plates, whereas the application of the sub-modelling is a must to investigate in detail the SB structural performances. In addition, results indicate that the BB attachments should be revised, as they contribute to produce the WCLL COB large deformation originating excessive stresses, mainly within the equatorial region.

## 1. Introduction

The breeding blanket (BB) is an essential component of the DEMO fusion reactor and its design is one of the pivotal purposes of the DEMO fusion reactor research [1–3]. Indeed, this component has to withstand severe operating conditions, as it is directly exposed to the plasma, making its design particularly challenging. In particular, the water-cooled lithium lead (WCLL) BB concept is one of the candidates currently considered for the conceptual design of the European DEMO reactor. In this context, Department of Engineering of the University of Palermo, as affiliated entity of ENEA, is involved in the design activities concerning the WCLL BB foreseen for DEMO nuclear fusion reactor supported by the EU community, within the Horizon2020 and Horizon

Europe framework programmes, carried out by the EUROfusion consortium.

The presented work is mainly focussed on the thermomechanical assessment of the central outboard blanket (COB) segment of the WCLL BB concept. The study of an entire segment is particularly onerous from both a computational and a modelling effort standpoint due to its size and the complexity of details it is made up. Therefore, in order to speed up the calculations and to make the mesh procedure easier, a complete assessment of the structural behaviour of the COB segment has been carried out [4] simplifying the model and removing some structural details, as the Segment Box cooling channels. In the above-mentioned work, the evaluation of the structural performances of some regions, as the toroidal-radial and poloidal-radial Stiffening Plates, in terms of

\* Corresponding author.

E-mail address: [ilenia.catanzaro@unipa.it](mailto:ilenia.catanzaro@unipa.it) (I. Catanzaro).

<https://doi.org/10.1016/j.fusengdes.2023.113601>

Received 30 November 2022; Received in revised form 10 February 2023; Accepted 21 February 2023

Available online 1 March 2023

0920-3796/© 2023 The Authors. Published by Elsevier B.V. This is an open access article under the CC BY license (<http://creativecommons.org/licenses/by/4.0/>).

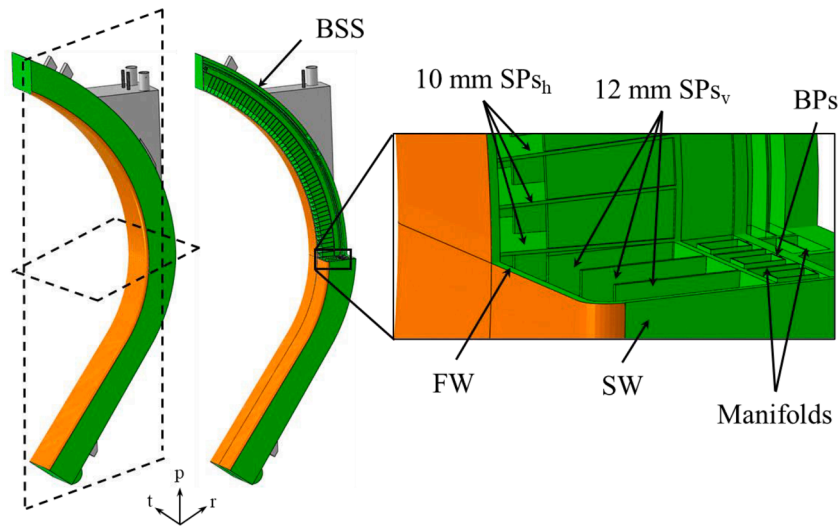


Fig. 1. WCLL COB segment architecture.

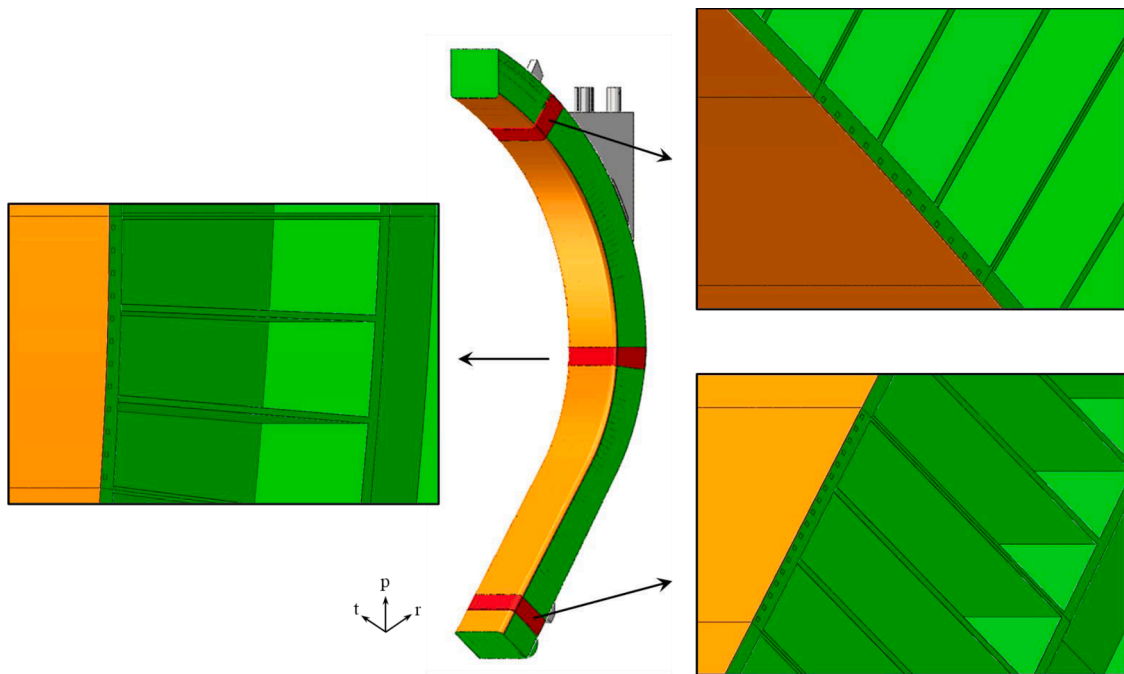


Fig. 2. Location of Top, Central and Bottom cells in the COB segment.

RCC-MRx design criteria fulfilment, has been presented.

Then, the present work is intended as a follow-up to the previous one [4]. Once investigated the overall structural behaviour of the WCLL COB segment under nominal and accidental loading scenarios, the sub-modelling technique has been adopted to assess in detail the structural performances of some regions of interest of the segment. Thanks to this approach, the local thermo-mechanical behaviour of some regions of the segment can be evaluated imposing, as boundary conditions, the displacement field previously calculated in the analysis of the whole segment. In this way, it is possible to impose at the border of the local models a set of boundary conditions directly drawn from the segment global analysis, so to take into account realistically the deformative effect imposed by the rest of the segment on the investigated regions. In particular, in this work, the sub-modelling technique is used to perform detailed analysis of the structural behaviour of the cooling channels region. Using the sub-modelling technique, it is then possible

to obtain the detailed stress level arising within local regions equipped with purposely designed cooling channels considering the effect of the rest of the segment as well as the loads acting on it. Moreover, the local analysis can rely on a finer mesh, allowing increasing the level of confidence of the results.

Therefore, 3D models reproducing three regions of the WCLL COB segment, consisting in a triplet of elementary cells located at three different poloidal heights, inserting the geometric entities not considered in the global model (i.e. cooling channels within the FW-SW) have been set-up. The thermomechanical analysis of the three sub-models under Normal Operation (NO), Over-Pressurization (OP) and Upper Vertical Displacement Event (UVDE) steady state scenarios have been performed with the aim of predicting the displacement and stress fields. Then, a stress linearization procedure has been performed along some paths located within the most stressed regions to verify the fulfilment of the RCC-MRx structural design criteria [5].

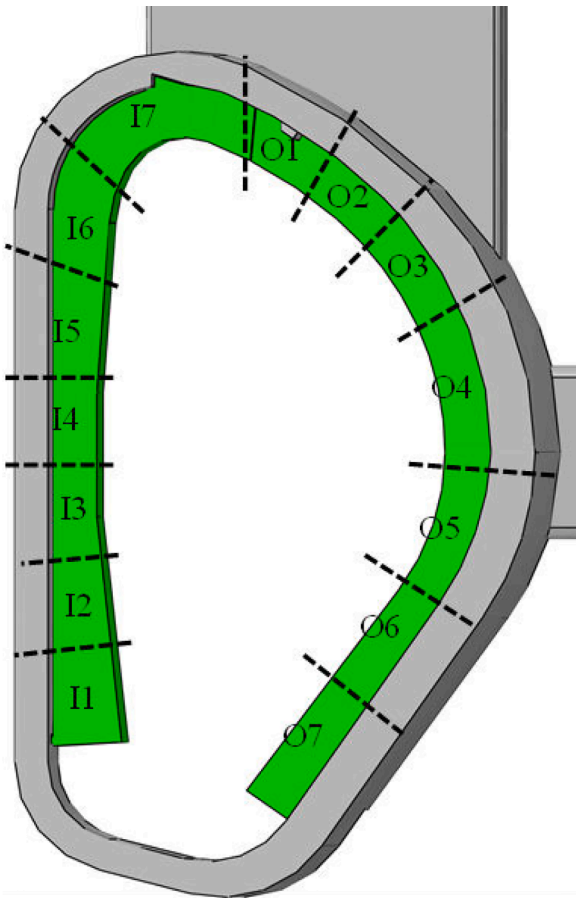


Fig. 3. DEMO BB poloidal segmentation and numbering.

Table 1  
Mesh features.

	Central Cells	Top Cells	Bottom Cells
Nodes	2 128 696	3 134 123	2 173 814
Elements	1 846 448	2 740 917	1 840 163

To this purpose, a theoretical-numerical approach based on the Finite Element Method (FEM) has been followed and the commercial code Abaqus v. 6.14 [6] has been used. The obtained results are here-with presented and critically discussed.

## 2. The WCLL COB segment

According to the DEMO baseline 2017 [7], 16 identical toroidal sectors are envisaged within the machine. Within each sector, 2 inboard (Left and Right, known as LIB and RIB respectively) and 3 outboard (Left, Central and Right indicated as LOB, COB and ROB respectively) segments can be identified. The COB segment (Fig. 1) is mainly constituted by an external steel structure, named Segment Box (SB), composed by First Wall (FW) and Side Walls (SWs) and closed vertically by upper and lower Caps. The SB is internally reinforced by a system of Stiffening Plates (SPs). In particular, the SPs are located along the poloidal-radial and toroidal-radial planes, namely horizontal (SP<sub>h</sub>) and vertical (SP<sub>v</sub>), and they are 10 mm and 12 mm thick, respectively. A 2 mm-thick Tungsten armour (coloured in orange in Fig. 1) coats the FW and an attachment system (in grey in Fig. 1), connected to a Back Supporting Structure (BSS), is foreseen in order to mechanically connect the SB to the Vacuum Vessel (VV). Moreover, a complex of Back Plates (BPs) and the water and breeder manifolds are located inside the steel structure.

The Lithium-Lead (PbLi), a liquid metal eutectic alloy acting as breeder and neutron multiplier, flows inside the SB, in the Breeder Zone (BZ), following a poloidal path thanks to a complex of Baffle Plates. Subcooled pressurized water, at the operational pressure of 15.5 MPa and an inlet/outlet temperature equal to 295/328 °C, flows inside bundles of Double Walled Tubes (DWTs), devoted to cool the BZ, and SB cooling channels having a square section.

In order to investigate the structural behaviour of the WCLL COB segment more in deep, since some details are absent in the global model analysis, the sub-modelling technique has been used to assess certain regions at different poloidal heights of the segment. In particular, a set of three elementary cells has been individuated within the upper, middle and lower part of the segment (highlighted in red in Fig. 2), belonging to O1, O4 and O7 region according to the poloidal segmentation showed in Fig. 3. Each model has been equipped with the proper cooling channel layout into the SW-FW-SW region, on the basis of the poloidal region they belong to: 4 channels for the upper and middle regions and 6 channels for the lower one, as reported in [3,4]. Neither Baffle Plates nor DWTs have been modelled because of their negligible structural role. Moreover, the PbLi, inside the Breeder Zone, and the water, flowing inside the cooling channels, have been not directly modelled but their effects have been appropriately considered thanks to a proper set of loads. The cells triplets have been obtained by cutting the whole COB model by means of plane passing through the middle of the upper and lower toroidal-radial SPs of each region, in order to obtain a wide physical interface in between the global and the local models to apply, by the sub-modelling technique, the proper displacement fields.

## 3. The FEM models

The three selected regions of the COB segment have been analysed from a structural standpoint under three steady state loading scenarios: NO, OP and UVDE. For each of the previously individuated 3D FEM models, a mesh has been obtained and a proper set of loads and boundary conditions have been selected and considered in order to reproduce each of the three loading scenarios.

### 3.1. The mesh

Concerning the meshes set-up for the three models, linear hexahedral elements have been used. Some mesh features are reported in Table 1 for each model. Moreover, the comparison between the mesh set-up in the sub-models with that of the global model in the analogous poloidal positions, reported in Fig. 4, highlights the increased level of detail of such a kind of analysis. For example, within the vertical and horizontal SPs thickness in the global model a number of elements equal to 1 and 2 are used respectively, instead, in the sub-models 6 and 8 elements are used within the same thicknesses. Indeed, thanks to a much finer mesh with respect to the one developed for the entire model analysis, it is possible to obtain for each sub-model a more detailed and accurate assessment, in particular, in terms of stress linearization results and the consequent evaluation of the RCC-MRx design criteria.

### 3.2. Loads and boundary conditions

The thermo-mechanical performances of the three models, representing the upper, middle and lower region of the WCLL COB segment, have been investigated under purposely selected steady state loading scenarios. First, the NO scenario has been considered. It takes into account the thermomechanical loads arising under the nominal operating condition (corresponding to the end of flat top plasma operational state) and therefore it is considered as Level A scenario in RCC-MRx structural design code. Then, analysis under the UVDE scenario have been performed. Such a scenario refers to an off-normal event due to a vertical plasma disruption, being classified as Level C. Lastly, the OP loading scenario has been considered. It refers to a severe accidental condition,

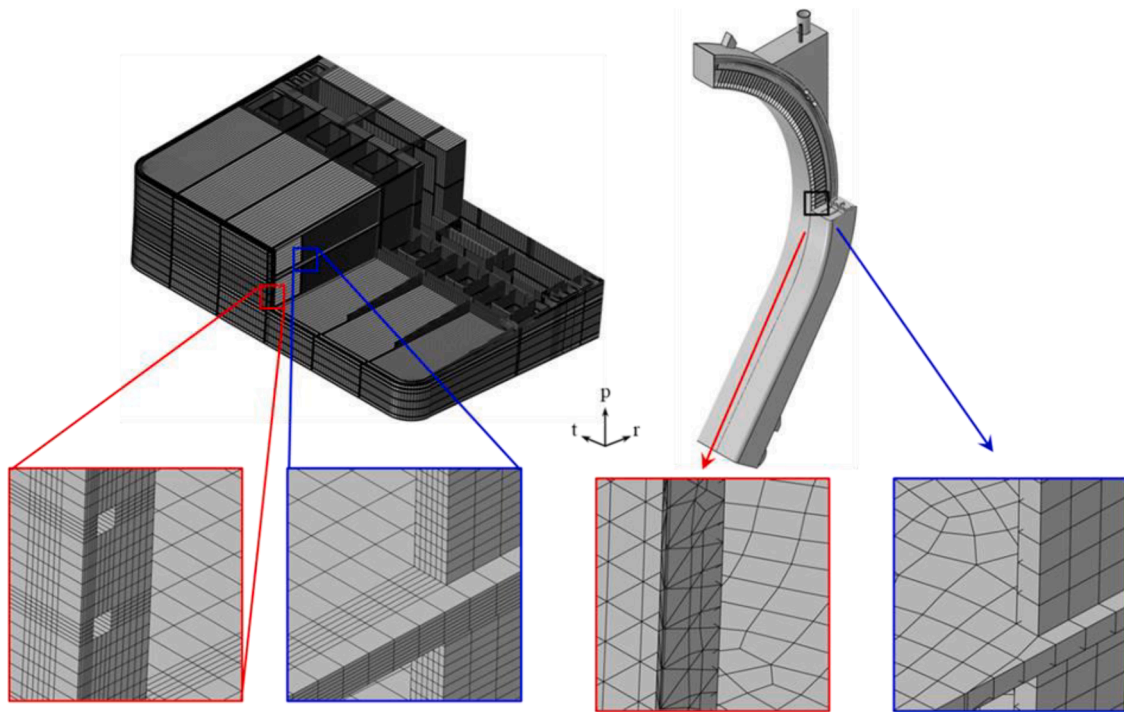


Fig. 4. Mesh of the CC sub-model vs mesh of the global model in the COB segment.

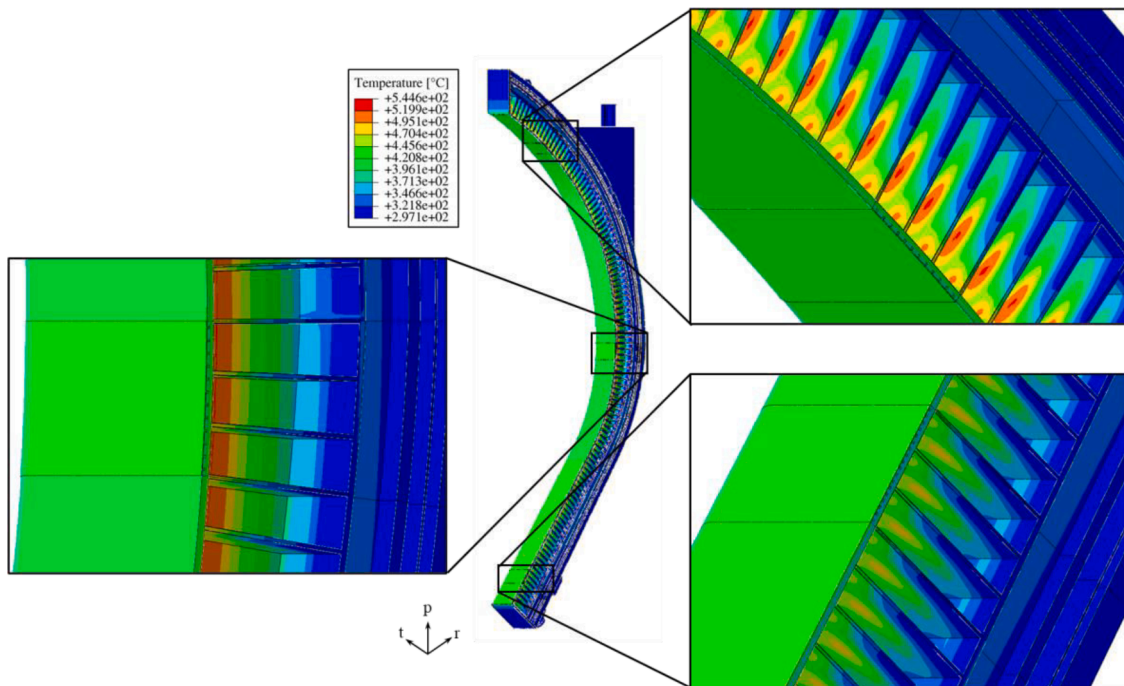


Fig. 5. Temperature field onto Top, Central and Bottom models superimposed to the global model.

relevant to a coolant leak within the segment that pressurizes the SB at the coolant pressure level, ultimately entailing the necessity to replace the component. It is hence classified under Level D in RCC-MRx structural design code. In order to correctly reproduce the NO, OP and UVDE loading scenarios, a proper set of loads and boundary conditions has been implemented.

In order to correctly reproduce these scenarios, the following loads and boundary conditions have been considered:

- thermal deformation field;
- gravity load;
- internal pressure distribution;
- electro-magnetic (EM) loads;
- mechanical restraints.

The thermal deformation field arising as consequence of the non-uniform temperature distribution has been considered. In particular, the thermal field obtained from the COB cooling layout optimization of



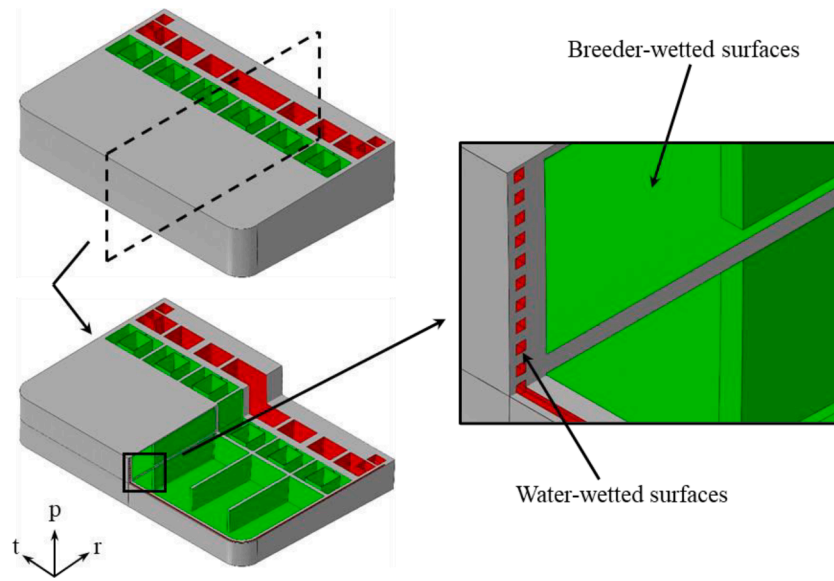


Fig. 6. Water and breeder wetted surfaces.

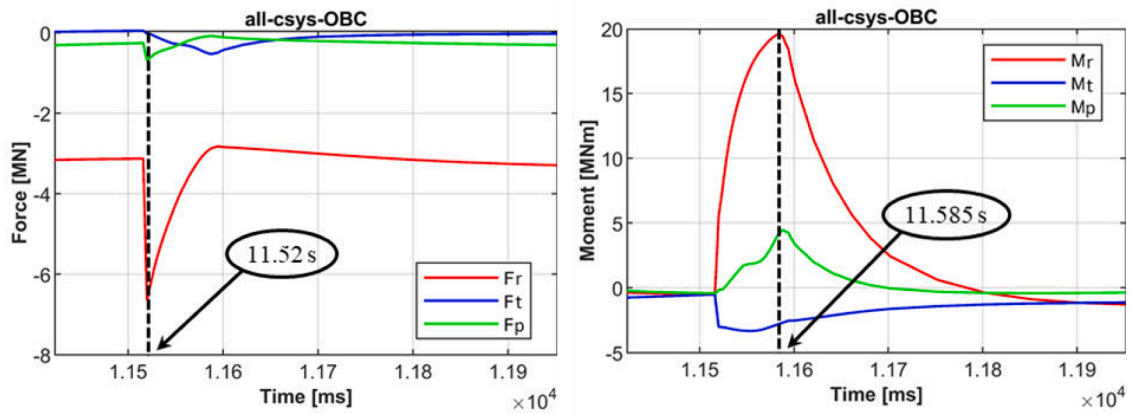


Fig. 7. Force and moment time behaviour during a VDE-up and maximum component (i.e. radial) time steps.

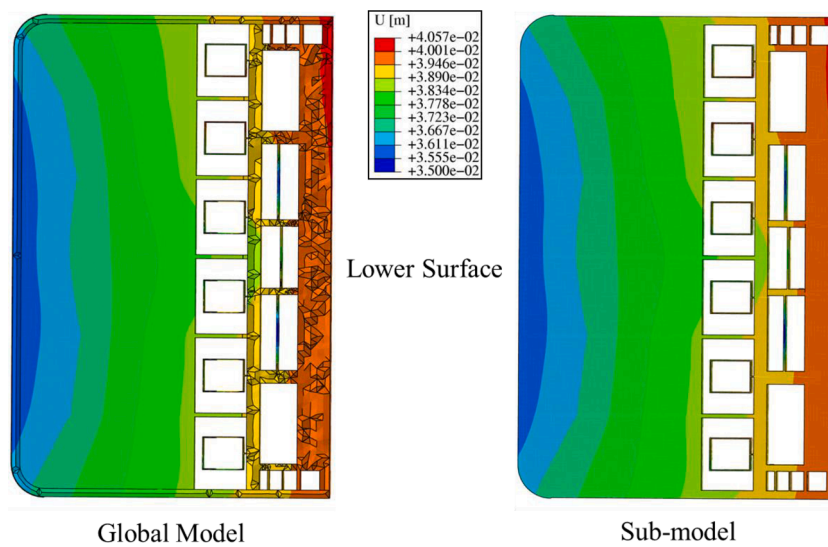


Fig. 8. Displacement field in global model and sub-model applied in NO scenario to the lower boundary of the central cells sub-model.

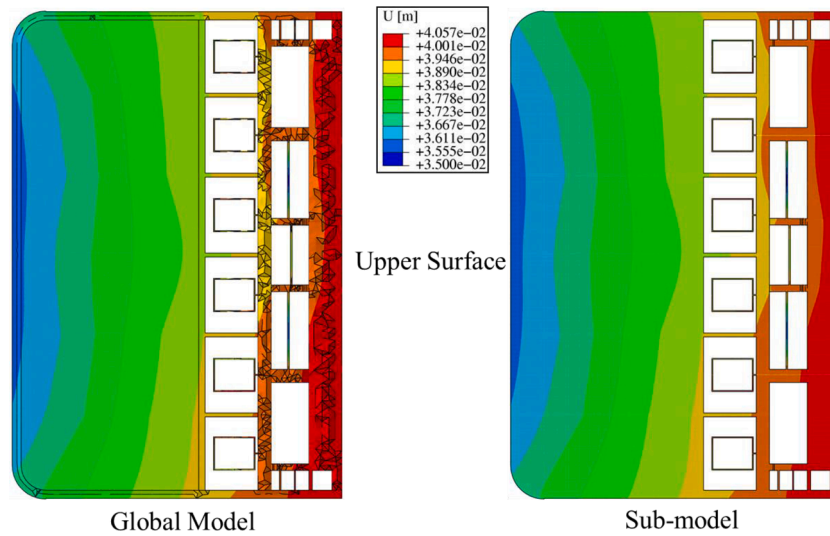


Fig. 9. Displacement field in global model and sub-model applied in NO scenario to the upper boundary of the central cells sub-model.

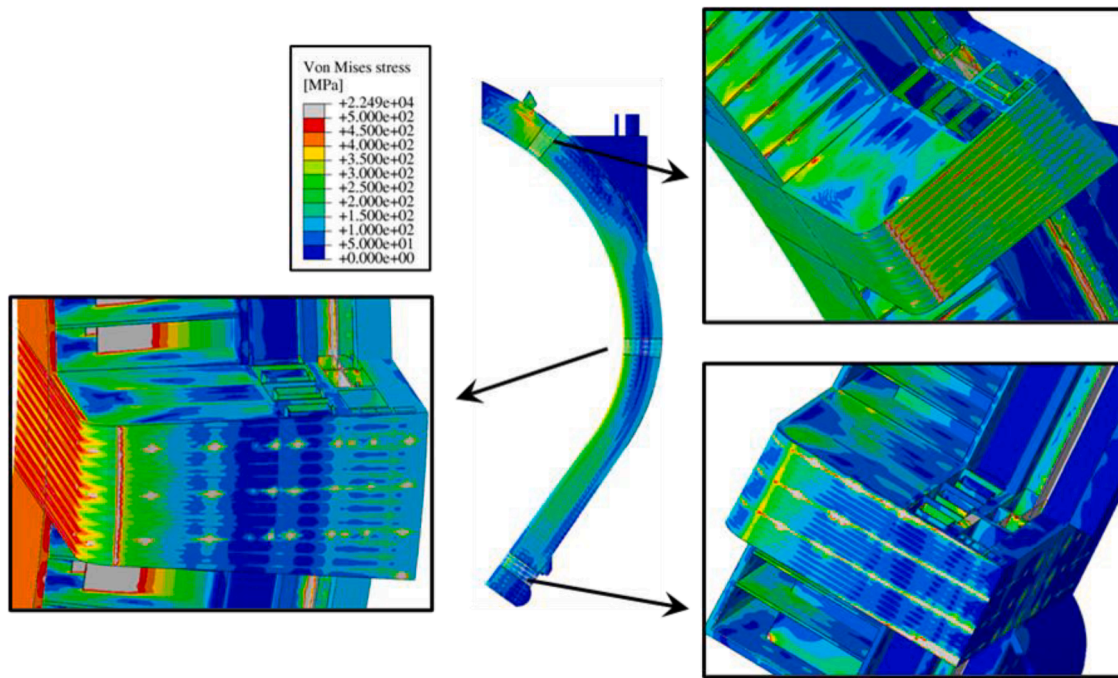


Fig. 10. Von Mises stress field within Top, Central and Bottom models in NO superimposed to the global model Von Mises stress field.

each poloidal region [4] and the following “multi-regions” interpolation [9], has been applied onto the three sub-models (Fig. 5).

The weight force has been taken into account imposing the gravity load to each model. Moreover, the Eurofer steel has been considered as structural material. Temperature dependant property for Eurofer and Tungsten have been adopted [10,11]. The density values have been properly modified in order to take into account the presence of breeder and water by means of a purposely calculated temperature-dependant equivalent density.

$$\rho_{eq}(T) = \frac{\sum_i \rho_i(T) \cdot V_i}{V_{tot}}$$

where  $\rho_i(T)$  is the temperature-dependant density of the  $i$  th material (steel, water or breeder) and  $V_i / V_{tot}$  is its volumetric fraction within the structure.

With regard to the internal pressure, as described in the BB Load

Specifications [8], to simulate the presence of the breeder and the coolant, in NO and UVDE loading scenarios a pressure of 17.825 MPa (equal to the nominal pressure 15.5 MPa increased by a factor of 1.15) has been imposed within every cooling channel inside the SW-FW-SW region. Moreover, a pressure of 0.575 MPa (the nominal value of 0.5 MPa increased by 1.15) has been considered for all the internal SB surfaces wetted by the breeder. During the OP loading scenario, as it represents a coolant leak event (LOCA accident), a pressure of 17.825 MPa has been applied onto both water and breeder-wetted surfaces. In Fig. 6 the breeder and water wetted surfaces are coloured in green and red, respectively.

The EM loads related to the NO, OP and UVDE scenarios have been taken into account. Since steady state analyses have been performed, the EM loads considered and used are relative to a specific instant of time, i. e., time step. In NO and OP scenarios, only the ferromagnetic loads contribution is considered. Instead, for the UVDE loading scenario, the

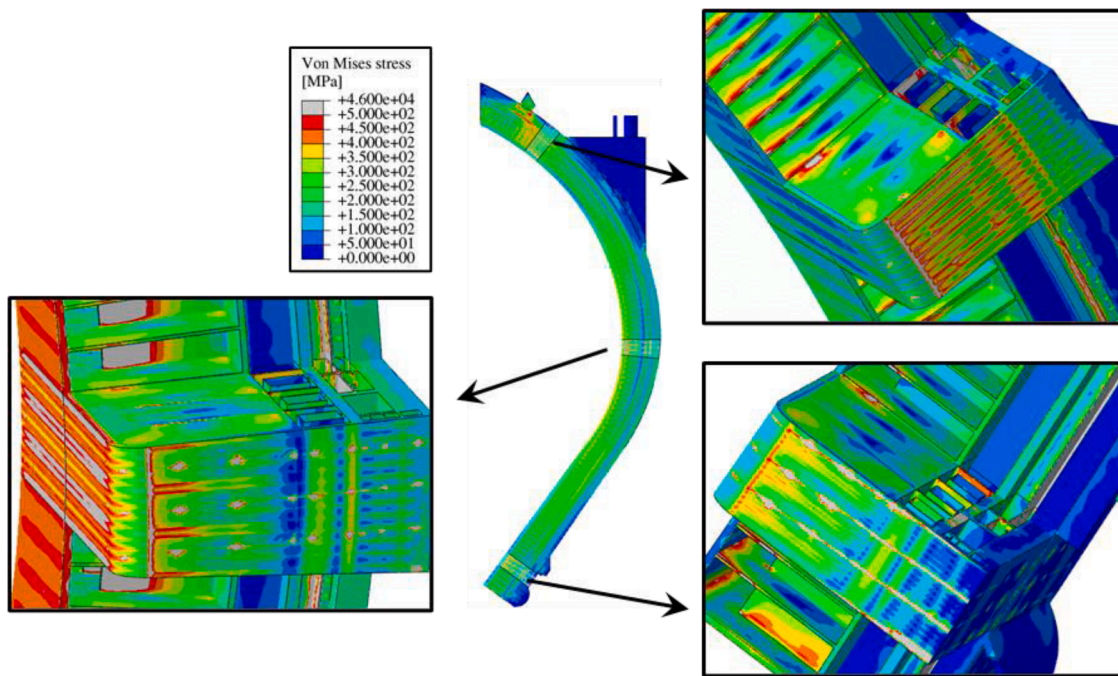


Fig. 11. Von Mises stress field within Top, Central and Bottom models in OP superimposed to the global model Von Mises stress field.

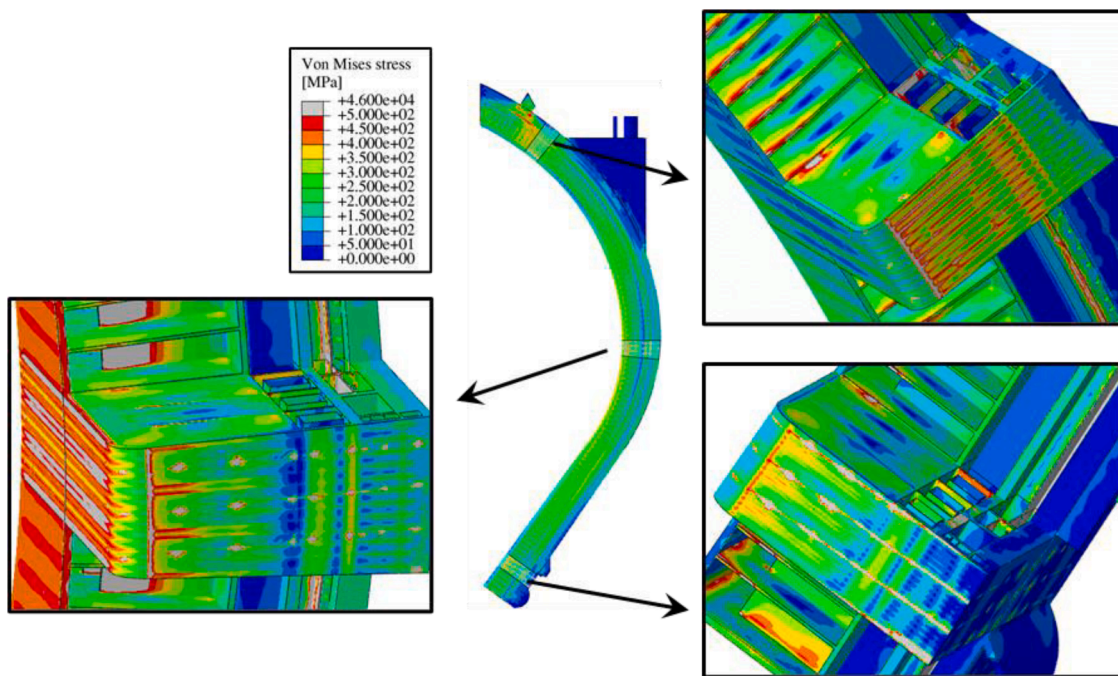


Fig. 12. Von Mises stress field within Top, Central and Bottom models in UVDE ( $t = 11.52$  s) superimposed to the global model Von Mises stress field.

accidental EM loads have been added to the ferromagnetic ones. As already done for the whole segment analysis [4], the EM loads of two different time steps have been considered for the UVDE scenario in order to perform steady state structural analysis. In particular, the selected time steps are relative to the maximum of the radial forces and moment,  $t = 11.52$  s and  $t = 11.585$  s respectively, as reported in Fig. 7. So, the EM loads, calculated by means of a dedicated electro-magnetic analysis [12], have been applied onto the node mesh of each sub-model thanks to a properly developed mesh-to-mesh matching procedure. This procedure allows to assign the EM force obtained at one point, individuated by a certain  $x, y, z$ , to the closest nodes of the developed mesh.

Finally, the sub-modelling technique in Abaqus consists in applying the displacements values along the three directions ( $u_r, u_t$  and  $u_p$ ) calculated in the respective regions of the global model to the nodes of the two cutting (i.e., boundary) surfaces of each sub-model. So, thanks to this technique, the analysed cells triplets take into account the thermo-mechanical response of the entire segment. Of course, the proper displacement spatial distribution has been applied depending on the loading scenario considered. As an example, in Figs. 8 and 9 the displacement field applied onto upper and lower faces in NO scenario for the central cells sub-model is depicted.



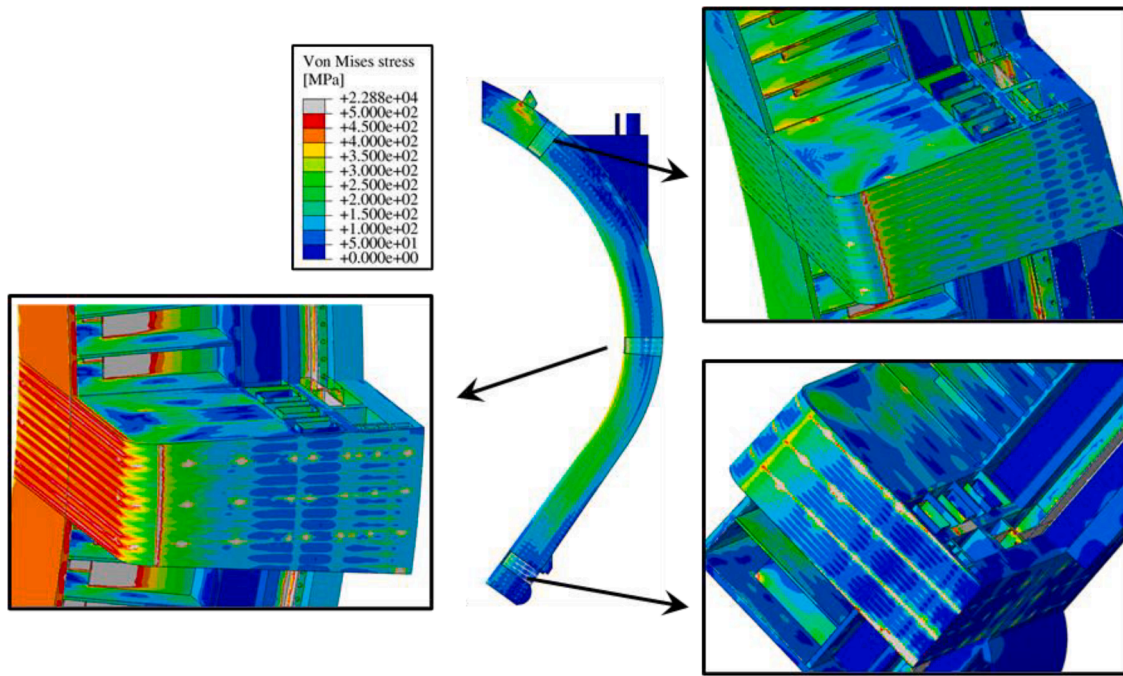


Fig. 13. Von Mises stress field within Top, Central and Bottom models in UVDE ( $t = 11.585$  s) superimposed to the global model Von Mises stress field.

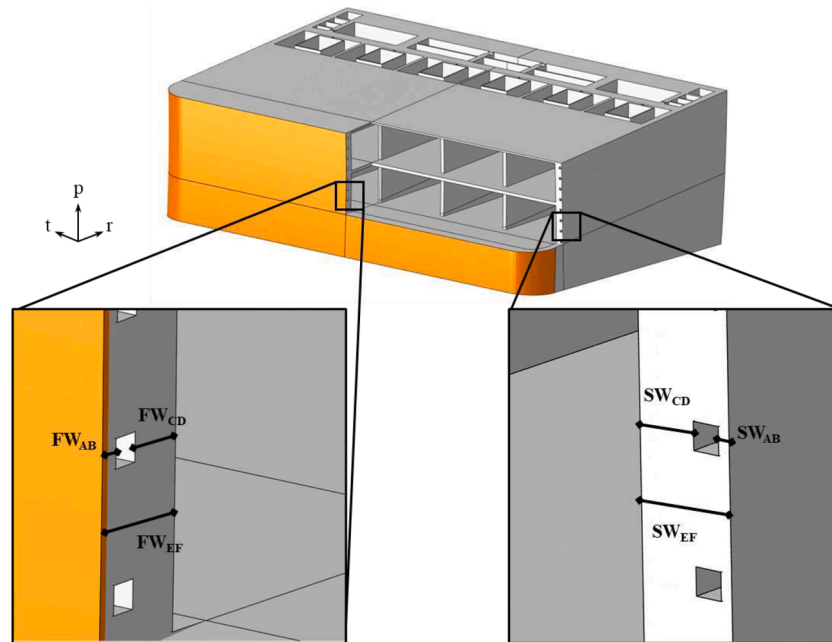


Fig. 14. Paths selected within FW-SW region in CC model.

#### 4. Results

Steady state analyses have been run in order to assess the thermo-mechanical behaviour of three particular regions of the WCLL COB segment under the selected NO, UVDE and OP loading scenarios, related to Level A, C and D service of level of RCC-MRx structural design code, respectively. In Figs. 10, 11, 12 and 13 the Von Mises equivalent stress field of the three regions analysed, namely Top, Central and Bottom cells, superimposed to the entire COB model response (calculated from the whole segment analysis), are depicted. Looking at these pictures, a very good continuity between stress calculated in the global model analysis and that obtained from sub-modelling analysis can be observed,

highlighting the capabilities of the adopted approach. Of course, the Von Mises stress distributions obtained from sub-modelling exhibits more details since the local models are endowed with SB cooling channels and are discretised with a finer mesh.

The obtained results have been analysed and a stress linearization procedure has been performed in order to verify of the fulfilment of the RCC-MRx design criteria corresponding to the Level A, Level C and Level D. Therefore, a proper set of paths has been selected, looking at the Von Mises equivalent stress field, in correspondence of the most stressed region of each model. In particular, localised peaks of Von Mises equivalent stress value occurring at the points of application of the electromagnetic forces should not be taken into account for the



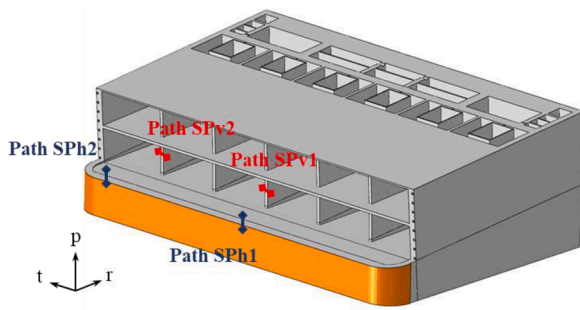


Fig. 15. Paths selected within SPs region in CC model.

Table 2  
RCC-MRx design criteria.

	Criteria
Immediate Excessive Deformation (IED)	$\frac{P_m}{S_{m,A-C-D}} < 1$
Immediate Plastic Instability (IPI)	$\frac{P_m + P_b}{K_{eff} \cdot S_{m,A-C-D}} < 1$
Immediate Plastic Flow Localization (IPFL)	$\frac{P_m + Q_m}{S_{em,A-C-D}} < 1$
Immediate Fracture due to exhaustion of ductility (IF)	$\frac{P_m + P_b + Q + F}{S_{et,A-C-D}} < 1$

evaluation of the RCC-MRx design criteria. As reported in Fig. 14, showing the paths selected in the Central Cells (CC) model, six paths have been selected within the FW and SW region. The same set of paths has been considered in the Top and Bottom Cells (TC and BC, respectively) models. Moreover, the same set of paths within the horizontal and vertical SPs already considered in the analysis of the whole segment have been adopted within the three sub-models. For the sake of brevity, in Fig. 15 only the considered paths within the SPs in the CC sub-models are reported, but the same set of paths has been considered for the BC and TC.

A stress linearization procedure has been performed and the equivalent stress value obtained within each path has been compared to the stress limits prescribed by the RCC-MRx design criteria. As already done, four criteria have been taken into account for the evaluation: immediate excessive deformation (IED), immediate plastic instability (IPI), immediate plastic flow localization (IPFL) and Immediate Fracture due to exhaustion of ductility (IF). In Table 2 the criteria are reported, where

$S_m$  is the maximum allowable primary membrane stress intensity of the material,  $S_{em}$  is the maximum allowable primary plus secondary membrane stress, function of temperature and irradiation,  $S_{et}$  is the maximum allowable total stress, also function of temperature and irradiation, and, finally,  $K_{eff}$  is a factor called “plastic collaboration coefficient”, equal to 1.5 for rectangular sections. Temperature-dependant values of  $S_m$ ,  $S_{em}$  and  $S_{et}$  have been differently calculated for Level A, C or D according to the structural material Eurofer properties. The stress limit values have been calculated at the path average temperature.

The obtained results have been summarized in Figs. 16, 17, 18 and 19, for the FW-SW region, and in Figs. 20, 21, 22 and 23, for the SPs, reporting the ratio between the equivalent stress values and the corresponding stress limits for each criterion.

Looking at the FW-SW region, results show that all the paths within the TC and BC regions fulfil the selected criteria, except for two paths (namely  $SW_{AB}$  and  $SW_{CD}$ ) with reference to the IPFL criterion (represented by the ratio  $(P_m + Q_m)/S_{em}$ ), in which it is not fulfilled or reaches high values ( $>0.8$ ). In particular, the IPFL criterion evaluated within the  $SW_{AB}$  path within the upper region of the segment is not fulfilled in NO, OP and UVDE ( $t = 11.52$  s) loading scenarios, far exceeding the limit. Beyond these exceptions, all of the selected criteria of the RCC-MRx design code evaluated along the other paths identified along the SW region are largely verified. Moreover, all the paths selected within the CC model fulfil the IED, IPI and IF criteria, instead all the paths on the FW region do not verify the criterion against the immediate plastic flow localization, taking into account the secondary stresses, reaching high values of the ratio.

Moreover, observing the results within the SPs, the same trend of results can be observed, in terms of RCC-MRx design criteria evaluation, compared to the global analysis results. In particular, the vertical SPs seem particularly stressed and the path SPv2 does not fulfil, or reaches high ratio values ( $>0.8$ ), the immediate plastic flow localization criterion, considering the secondary stresses, in each sub-model and in every loading scenario considered. This result is attributable to a higher average temperature value with respect to the other paths located within the vertical SPs (i.e. SPv1).

In conclusion, the verification of the RCC-MRx criteria has allowed confirming the results obtained from the global analysis of the whole segment. In fact, the most critical region is still the equatorial one, where a remarkable radial deformation arises due to the geometric layout of the attachment system. In the other regions, the predicted structural behaviour seems to be promising. Hence, a deep revision of the geometric configuration of the attachments seems to be helpful in order to reduce the stress level within the WCLL COB segment, not only within

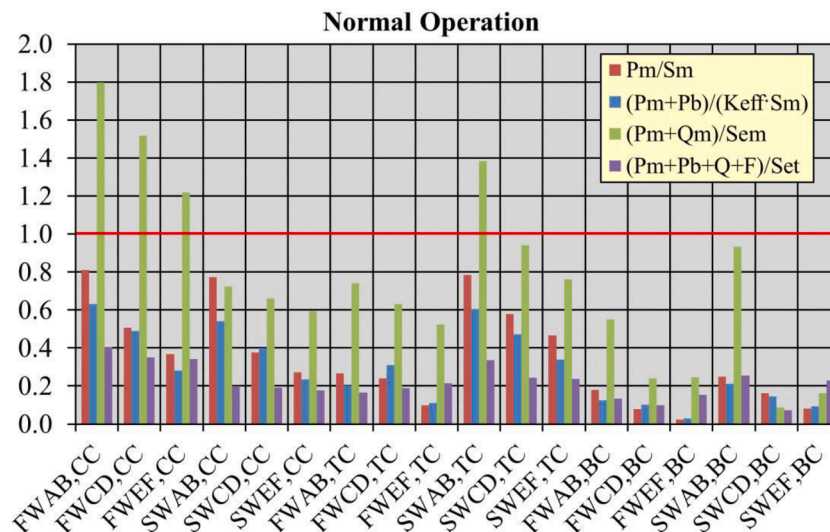


Fig. 16. RCC-MRx criteria verification in NO loading scenario within FW-SW.

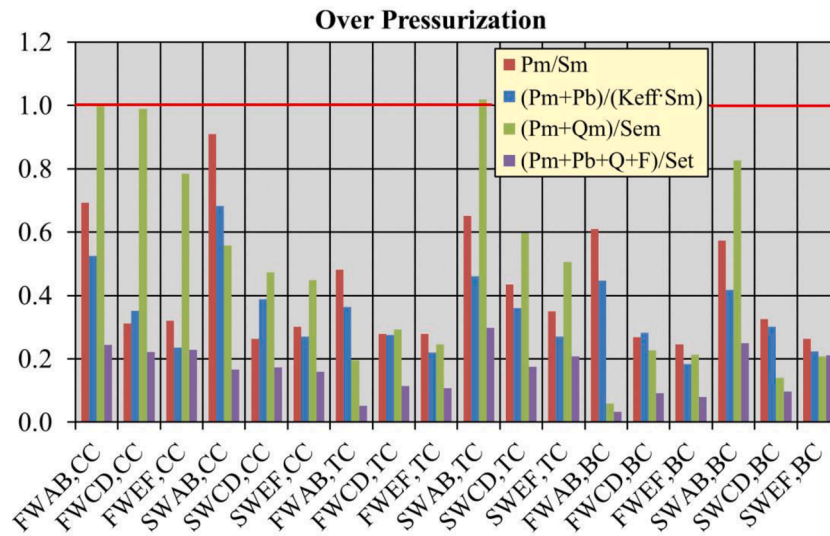


Fig. 17. RCC-MRx criteria verification in OP loading scenario within FW-SW.

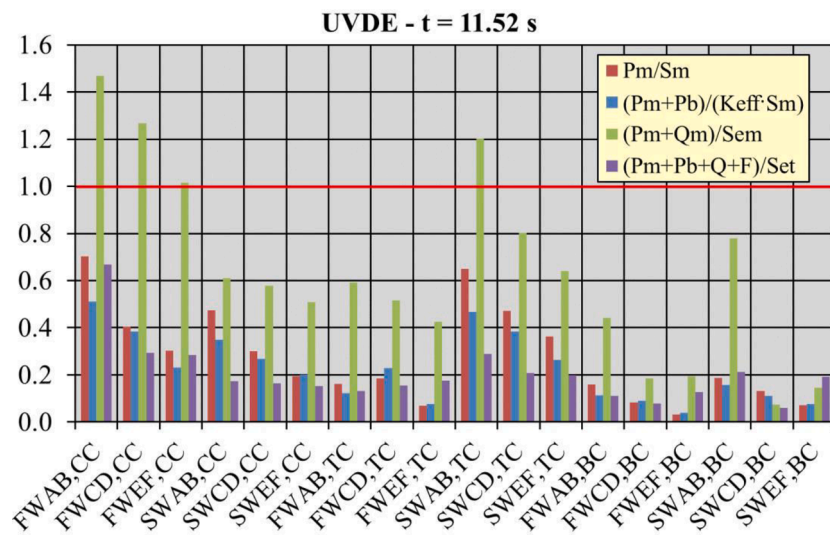


Fig. 18. RCC-MRx criteria verification in UVDE ( $t = 11.52$  s) loading scenario within FW-SW.

SPs but also within the FW-SWs regions. A system of attachment including an equatorial support could be helpful to contain large radial displacements predicted in the equatorial region and also to reduce high stresses.

In addition, it can be observed that comparing the results of the stress linearization and the evaluation of the RCC-MRx design criteria obtained along the same SPs paths, when the stresses are evaluated in the global and in the sub-models, a very similar behaviour is found. The whole set of comparisons are not reported in this work for the sake of brevity. As an example, the comparison between the results of the RCC-MRx criteria verification along the same SPs paths within the global model (GM) and the CC sub-model (SM) in NO loading scenario is reported in Fig. 24. The other results, in OP and UVDE loading scenarios and within the BC and TC, show a similar trend and are not reported here for the sake of brevity. Therefore, since a similar behaviour is observed, this allows concluding that, in the sub-modelling analysis, the attention and the modelling effort can be focussed on the FW-SWs region since the global analysis already provides reliable results concerning the SPs domain.

The percentage errors of the ratio, previously defined, for the NO loading scenario in the CC sub-model is reported in Table 3. In any way,

a similar trend can be observed for each loading scenario and within the three analysed regions, here not reported for brevity. Such percentage of error is calculated as the difference between the ratio value assessed within each path in the global model analysis and in the sub-models divided by the first. In particular, percentage errors are sometimes very high because the results are strongly dependant on the density of the grid used but it can be observed that the highest values of percentage error are predicted where the ratio values are the lowest. Globally, the results show that the thermo-mechanical behaviour derived by the analysis of the entire model provides a reliable response in terms of design criteria verification when compared with a more in-depth analysis performed by means of the sub-modelling technique.

Moreover, the same comparison, between the RCC-MRx criteria evaluated within the global model and the sub-models, has been performed along the paths “FW EF” and “SW EF”, selected within the FW-SW region between two cooling channels. Indeed, although the cooling channels within the SB have not been modelled in the global model, it is possible to obtain the structural response in that region of the FW-SW, not occupied by channels, and compare it with that of a more detailed model.

In Table 4 the results in terms of percentage of error for each NO

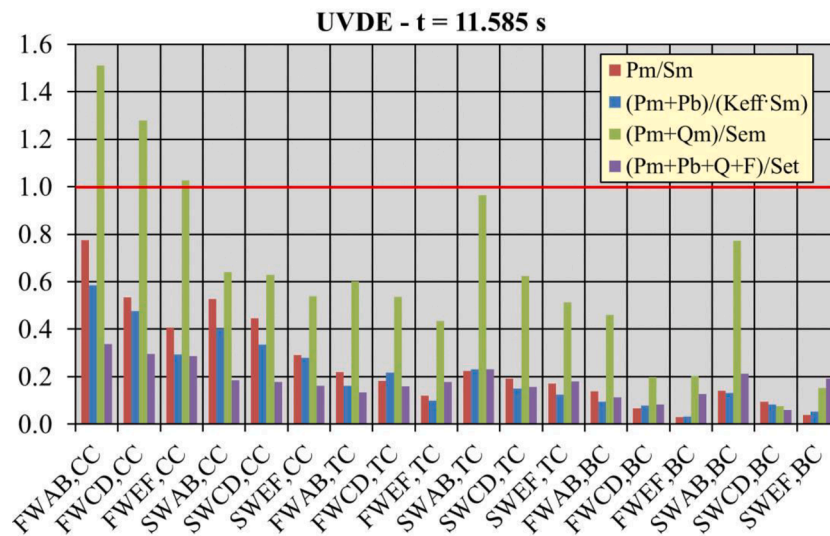


Fig. 19. RCC-MRx criteria verification in UVDE ( $t = 11.585$  s) loading scenario within FW-SW.

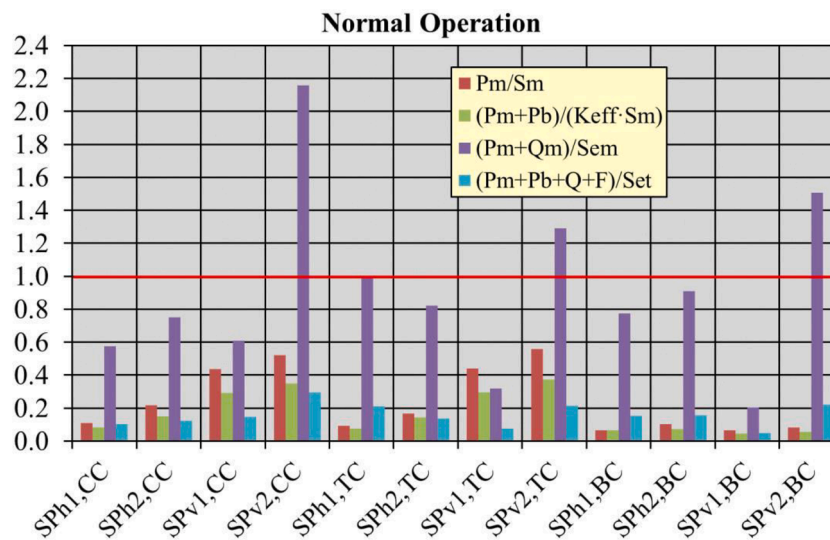


Fig. 20. RCC-MRx criteria verification in NO loading scenario within SPs.

criterion evaluated along the “FW EF” and “SW EF” paths within the three poloidal regions are reported. In particular, it can be observed that globally the error is higher than that obtained when the comparison is performed within the SPs paths. However, the most interesting aspect to point out is that a much larger error is obtained when these paths are evaluated in the bottom part of the segment (BC), and, in particular, in that criterion taking into account the peak stresses (IF). In fact, in that region 6 cooling channels are expected. This trend suggests that in those regions provided of 4 cooling channels, the “EF” paths are barely influenced by the channels, due to the greater amount of steel between them. On the contrary, where 6 channels are expected, the distance between them is smaller and the regions are more effected by them. Hence, it can be concluded that global model analyses provide structural results with a good accuracy, in terms of RCC-MRx design criteria, when regions far from the cooling channels are investigated, as can be expected. In any case, the sub-modelling technique is always necessary in order to take into account the channels effect and to in-depth study the region immediately next to them (AB and CD paths).

### 5. Conclusion

Within the framework of the research activities regarding the European DEMO Breeding Blanket, a study has been carried out in order to assess the thermo-mechanical behaviour of the DEMO WCLL COB segment under different loading scenarios, in view of the RCC-MRx design criteria, paying attention to the SB endowed with its cooling channels.

In particular, the performed activity aims to study in detail the structural performances in some regions of interest of the COB segment, adopting the sub-modelling technique. An upper, a central and a lower triplet of cells of the WCLL COB segment have been investigated with a high level of detail, considering a FW-SW region equipped with the corresponding cooling channels.

Results, in terms of fulfillment of the RCC-MRx design criteria, show that the equatorial region of the segment is the most stressed, as already obtained in the analysis of the entire segment where the attention was focused on the SPs domain, whereas no particular concerns arise for upper and lower regions of the segment. Therefore, these outcomes suggest a revision of the attachment system, in order to reduce the large displacements and the high stress level occurring in that region.

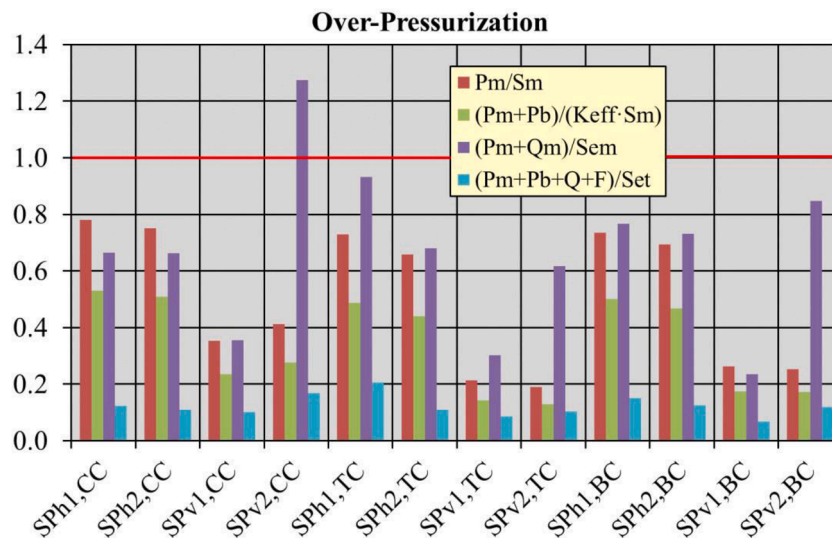


Fig. 21. RCC-MRx criteria verification in OP loading scenario within SPs.

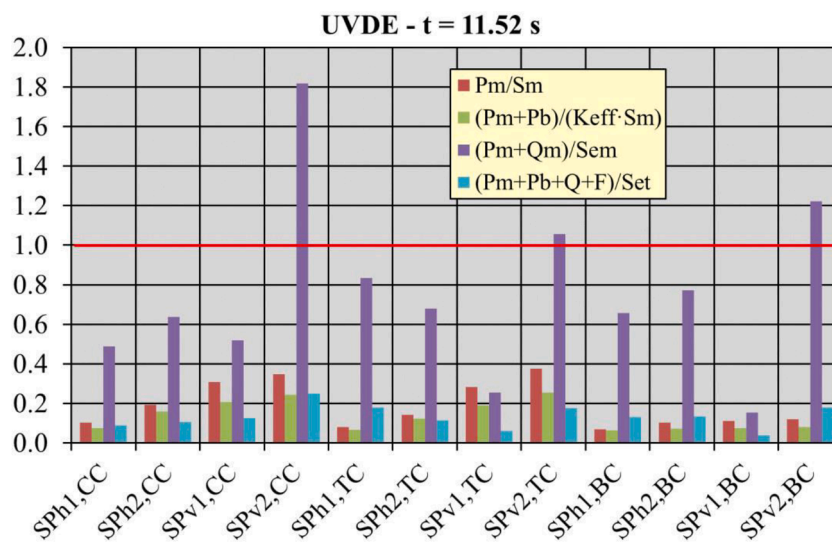


Fig. 22. RCC-MRx criteria verification in UVDE ( $t = 11.52$  s) loading scenario within SPs.

Moreover, from the comparison between the stress linearization results obtained along the same paths in the global model and in the sub-models a similar behaviour can be observed. In general, it can be stated that the in-depth study of SB regions that have been simplified in the global model (i.e., the FW-SW region) is possible thanks to the sub-modelling technique, instead the thermomechanical response of the SPs is rather similar in both analyses and is therefore not strictly dependant on the mesh used. Thus, the structural behaviour of the SPs can be predicted with good accuracy already in the global model analyses and, therefore, it is not necessary to study them in detail in the sub-models' analyses. For this reason, a coarser mesh within the SPs could be adopted in the sub-model, while it is possible to increase the mesh density in particular regions, as the FW-SW, in order to reduce the computational burden and, at the same time, obtaining accurate results.

**CRedit authorship contribution statement**

**I. Catanzaro:** Formal analysis, Writing – original draft, Conceptualization, Methodology, Investigation, Resources, Data curation, Writing – review & editing, Visualization. **G. Bongiovi:** Formal analysis, Writing – original draft, Conceptualization, Methodology, Investigation,

Resources, Data curation, Writing – review & editing, Visualization. **P.A. Di Maio:** Supervision, Project administration, Funding acquisition, Conceptualization, Methodology, Investigation, Resources, Data curation, Writing – review & editing, Visualization. **P. Arena:** Conceptualization, Methodology, Investigation, Resources, Data curation, Writing – review & editing, Visualization. **G.A. Spagnuolo:** Conceptualization, Methodology, Investigation, Resources, Data curation, Writing – review & editing, Visualization.

**Declaration of Competing Interest**

The authors declare that they have no known competing financial interests or personal relationships that could have appeared to influence the work reported in this paper.

**Data availability**

No data was used for the research described in the article.



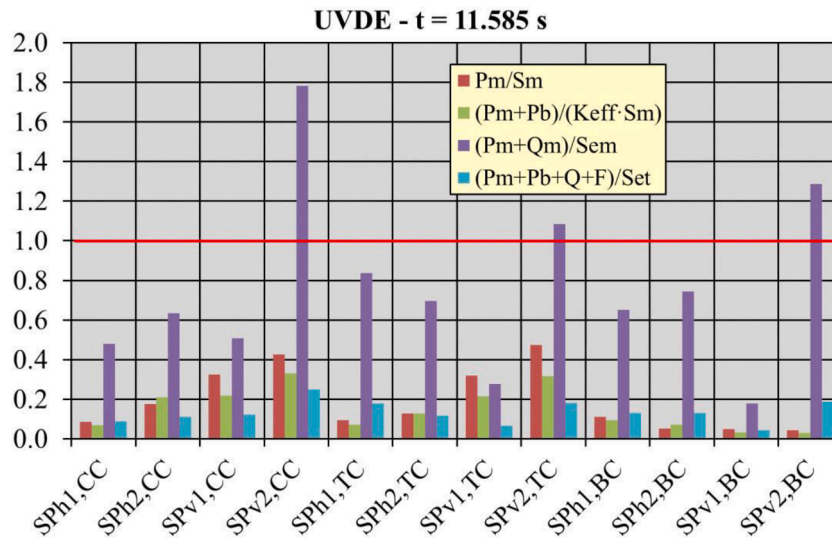


Fig. 23. RCC-MRx criteria verification in UVDE ( $t = 11.585$  s) loading scenario within SPs.

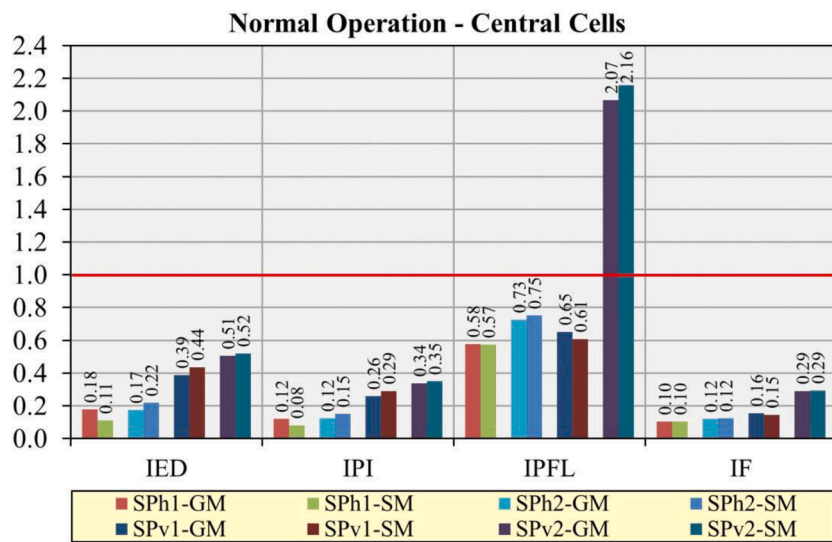


Fig. 24. RCC-MRx criteria evaluation within global model and CC sub-model in NO scenario.

Table 3

RCC-MRx NO criteria percentage errors global model vs sub-model in CC.

	E%(IED)	E%(IPI)	E%(IPFL)	E%(IF)
SPh1	38.63%	31.79%	0.61%	-0.41%
SPh2	-24.87%	-21.31%	-3.36%	-3.26%
SPv1	-12.39%	-12.38%	6.54%	6.64%
SPv2	-2.84%	-3.51%	-4.45%	-1.09%

Table 4

RCC-MRx NO criteria percentage errors global model vs sub-model within “FW EF” and “SW EF” paths.

	E%(IED)	E%(IPI)	E%(IPFL)	E%(IF)
FW EF <sub>CC</sub>	20.26%	21.94%	14.47%	-21.38%
SW EF <sub>CC</sub>	19.31%	5.27%	1.94%	-19.66%
FW EF <sub>TC</sub>	14.98%	-4.93%	19.52%	-51.61%
SW EF <sub>TC</sub>	11.20%	4.95%	6.93%	-15.58%
FW EF <sub>BC</sub>	61.38%	30.08%	22.80%	-108.80%
SW EF <sub>BC</sub>	30.93%	-14.02%	-21.44%	-197.17%

### Acknowledgement

This work has been carried out within the framework of the EUROfusion Consortium, funded by the European Union via the Euratom Research and Training Programme (Grant Agreement No 101052200 — EUROfusion). Views and opinions expressed are however those of the author(s) only and do not necessarily reflect those of the European Union or the European Commission. Neither the European Union nor the European Commission can be held responsible for them.

### References

- [1] L.V. Boccaccini, et al., Status of maturation of critical technologies and systems design: breeding blanket, Fusion Engin. Des. Volume 179 (June 2022), 113116, <https://doi.org/10.1016/j.fusengdes.2022.113116>.
- [2] T. Donnè, European research roadmap to the realisation of fusion energy, November 2018, ISBN: 9783000611520.
- [3] P. Arena, et al., The DEMO water-cooled lead-lithium breeding blanket: design status at the end of the Preconceptual design phase, Appl. Sci. 11 (24) (2021) 11592, <https://doi.org/10.3390/app112411592>.
- [4] I. Catanzaro, et al., Analysis of the thermo-mechanical behaviour of the EU DEMO water-cooled lithium lead central outboard blanket segment under an optimized

- thermal field, *Appl. Sci.* 12 (3) (2022) 1356, <https://doi.org/10.3390/app12031356>.
- [5] RCC-MRx, *Design and Construction Rules For Mechanical Components of Nuclear Installations*, AFCEN, Courbevoie, France, 2013.
- [6] *Abaqus Analysis User's Guide: Online Documentation; Version 6.14-2*, Dassault System, Simulia: Providence, RI, USA, 2015.
- [7] R. Wenninger, DEMO1 reference design - 2017 March ("EU DEMO1 2017"), IDM Ref. EFDA\_D\_2NE9JA, 19 June 2017.
- [8] G.A. Spagnuolo, et al., Development of load specifications for the design of the breeding blanket system, *Fusion Engin. Des.* 157 (2020), 111657, <https://doi.org/10.1016/j.fusengdes.2020.111657>.
- [9] I. Catanzaro, et al., Development and application of an alternative modelling approach for the thermo-mechanical analysis of a DEMO water-cooled lithium lead breeding blanket segment, *Fusion Engin. Des.* 180 (2022), 113195, <https://doi.org/10.1016/j.fusengdes.2022.113195>.
- [10] E. Gaganidze, *Material Properties Handbook – EUROFER97* (2020), EFDA IDM Ref. EFDA\_D\_2NZHBS.
- [11] E. Gaganidze, F. Schoofs, *Material Properties Handbook – Tungsten* (2020), EFDA IDM Ref. EFDA\_D\_2P3SPL.
- [12] I.A. Maione, et al., A complete EM analysis of DEMO WCLL breeding blanket segments during VDE-up, *Fusion Engin. Des.* Volume 146 (2019) 198–202, <https://doi.org/10.1016/j.fusengdes.2018.12.017>.